

# Generation and Suppression of Decoherence in Artificial Environment for Qubit System

Yasushi Kondo<sup>1</sup>, Mikio Nakahara<sup>1\*</sup>, Shogo Tanimura<sup>2</sup>, Sachiko Kitajima<sup>3</sup>, Chikako Uchiyama<sup>4</sup>, and Fumiaki Shibata<sup>5</sup>

<sup>1</sup>*Department of Physics, Kinki University,  
Higashi-Osaka 577-8502, Japan*

<sup>2</sup>*Graduate School of Engineering, Osaka City University,  
Sumiyoshi-ku, Osaka 558-8585, Japan*

<sup>3</sup>*Graduate School of Pure and Applied Sciences,  
University of Tsukuba, Tenodai 1-1-1 Tsukuba,  
Ibaraki 305-8571 Japan*

<sup>4</sup>*Faculty of Engineering, University of Yamanashi,  
4-3-11 Takeda, Kofu, Yamanashi 400-8511, Japan*

<sup>5</sup>*Department of Physics, Faculty of Science,  
Ochanomizu University, Tokyo 112-8610, Japan*

(Dated: February 9, 2020)

It is known that a quantum system with finite degrees of freedom can simulate a composite of a system and an environment if the state of the hypothetical environment is randomized by external manipulation. We show theoretically that any phase decoherence phenomena of a single qubit can be simulated with a two-qubit system and demonstrate experimentally two examples: one is phase decoherence of a single qubit in a transmission line, and the other is that in a quantum memory. We perform NMR experiments employing a two-spin molecule and clearly measure decoherence for both cases. We also verify experimentally that the bang-bang control efficiently suppresses decoherence.

PACS numbers: 03.65.Yz, 03.67.-a, 03.67.Pp, 82.56.Na

Keywords: NMR quantum computer, channel, decoherence, bang-bang control

## I. INTRODUCTION

Quantum computing currently attracts a lot of attention since it is expected to solve some of computationally hard problems for a conventional digital computer [1]. Numerous realizations of a quantum computer have been proposed to date. Among others, a liquid-state nuclear magnetic resonance (NMR) quantum computer is regarded as most successful. Demonstration of Shor's factorization algorithm with NMR is one of the most remarkable achievements [2]. Liquid state NMR will be denoted simply as NMR throughout this paper.

Although the current NMR quantum computer is suspected not to be a true quantum computer because of its poor spin polarization at room temperature [3], it still works as a test bench for a more realistic quantum computer. For example, we have demonstrated our time-optimal implementation of two-qubit quantum algorithms by using an NMR quantum computer [4, 5].

A molecule employed in NMR experiments can be arranged to work not only as a quantum register but also as a composite system of a quantum system and its environment. It is possible to introduce decoherence phenomena in the quantum subsystem by manipulating the environment subsystem. Moreover the combined system can be employed as a test bench to develop techniques to pro-

tect a quantum system from decoherence. Decoherence is one of the primary obstacles in constructing a working quantum computer and must be suppressed somehow. Decoherence effect in a quantum register has also been studied elsewhere [6].

The main purpose of this paper is two fold. Firstly, we show that decoherence can be generated by manipulating the artificial environment. Secondly, we verify by NMR experiments that decoherence control methods, such as a bang-bang control [7, 8], actually suppress decoherence. It should be noted that demonstration of the effectiveness of decoherence control methods is rather difficult in other systems due to their extremely short coherence time. We note that spin relaxation induced by experimentally generated classical random field has been analyzed by Kohmoto *et al.* [9].

Section II is a brief review of the theory of quantum channel, which is a useful formalism to describe decoherence in a general context. In Section III we describe decoherence of a one-qubit system in terms of the quantum channel. There we discuss the method to suppress decoherence by a bang-bang control. In Section IV we show that a two-qubit system may be regarded as a composite of a system (qubit 1) and an environment (qubit 2). We realize an artificial environment by manipulating qubit 2, which causes decoherence in qubit 1. We show two illustrating examples and calculate decoherence rates in these environments. We also show that application of a bang-bang control to qubit 1 suppresses the decoherence. In Section V we report the results of our experiments, which support our theory. Using a two-spin molecule we demon-

---

\*Also at Low Temperature Laboratory, Helsinki University of Technology, Box 2200, 02015 TKK, Finland

strate the generation of decoherence and its suppression by the bang-bang control. Section VI is devoted to conclusions.

## II. DECOHERENCE

### A. Quantum Channel

Decoherence is an irreversible change of a state of a quantum system which has correlation with its environment. The change of the state of the system becomes irreversible due to our lack of knowledge about the state of the environment.

Decoherence is formulated in terms of channel or quantum operation [1, 10, 11, 12] as follows. Let  $\mathcal{H}_s$  and  $\mathcal{H}_e$  be the Hilbert spaces of the system and the environment, respectively. The initial state of the system is represented by the density matrix  $\rho_s$  while that of the environment by  $\rho_e$ . The state of the whole system changes following the time-evolution law,

$$\rho_s \otimes \rho_e \rightarrow U \rho_s \otimes \rho_e U^\dagger. \quad (1)$$

Here  $U$  is a unitary operator acting on the Hilbert space of the composite system  $\mathcal{H}_s \otimes \mathcal{H}_e$ . The states of the system and the environment are correlated via the transformation (1). Needless to say, the unitary transformation (1) is a reversible change. If we are interested only in the state of the system, the measurement outcomes are completely described by the reduced density matrix

$$\rho'_s = \mathcal{E}(\rho_s) = \text{Tr}_e \left( U \rho_s \otimes \rho_e U^\dagger \right), \quad (2)$$

where the symbol  $\text{Tr}_e$  denotes the partial trace over  $\mathcal{H}_e$ . The partial trace operation is noninvertible and the associated loss of information leads to decoherence. Even if the initial state  $\rho_s$  is a pure state, the transformed state  $\mathcal{E}(\rho_s)$  becomes a mixed state in general.

The mapping  $\rho_s \rightarrow \mathcal{E}(\rho_s)$  is called a channel or a quantum operation [1]. A channel is the most general mathematical device to describe changes of a quantum state, including unitary time-evolution, measurement process, decoherence and so on. It is known that for a channel there is a set of operators  $\{E_k\}$  acting on  $\mathcal{H}_s$  such that

$$\mathcal{E}(\rho_s) = \sum_k E_k \rho_s E_k^\dagger, \quad (3)$$

$$\sum_k E_k^\dagger E_k = I_s. \quad (4)$$

Here  $I_s$  is the identity operator on  $\mathcal{H}_s$ . Equation (3) is called an operator-sum representation of the channel  $\mathcal{E}$ . Equation (4) implies  $\text{Tr}_s \mathcal{E}(\rho_s) = \text{Tr}_s \rho_s$  and hence it is called the trace-preserving condition.

### B. Mixing process as a quantum channel

There is another approach to defining channels without resort to partial trace over the Hilbert space of environment. Assume that we have a set of unitary operators  $\{U_k\}$ , which act on  $\mathcal{H}_s$ , and that we have a set of real numbers  $\{p_k\}$  such that  $0 \leq p_k \leq 1$  and  $\sum_k p_k = 1$ . We then define a transformation of the system density matrix  $\rho_s$  by

$$\rho_s \rightarrow \mathcal{M}(\rho_s) = \sum_k p_k U_k \rho_s U_k^\dagger. \quad (5)$$

They satisfy the condition (4) if we put  $E_k = \sqrt{p_k} U_k$ . This argument tells us that if we apply a set of time-evolution unitary operators  $\{U_k\}$  on the system with a probability distribution  $\{p_k\}$ , we will observe a decoherence-like phenomenon after taking an average of the measured data. We call the transformation  $\mathcal{M}$  a mixing process.

Although a mixing process is defined superficially without referring to an environment, it is mathematically a special case of a channel that is defined through interaction between a system and an environment. For given sets of unitary operators  $\{U_k\}$  and probabilities  $\{p_k\}$ , we can construct a Hilbert space  $\mathcal{H}_e = \{ \sum_k c_k |k\rangle \}$  by demanding formally that  $\{|k\rangle\}$  is a complete orthonormal set. Moreover, we can define an environment density matrix

$$\rho_e = \sum_k p_k |k\rangle \langle k| \quad (6)$$

and define a unitary operator  $U = \sum_k U_k \otimes |k\rangle \langle k|$  that acts on  $\mathcal{H}_s \otimes \mathcal{H}_e$  as

$$U(|\psi_s\rangle \otimes |k\rangle) = (U_k |\psi_s\rangle) \otimes |k\rangle. \quad (7)$$

By substituting them into the defining equation of channel (2), we get the mixing process (5). In this paper we use the mixing process as a procedure to build a channel.

## III. DECOHERENCE IN ONE-QUBIT SYSTEM

### A. Phase flip channel

Here we introduce the phase flip channel, which is a typical example of a channel. We take a one-qubit system and a one-qubit environment. Assume that the initial state of the environment is

$$|\psi_e\rangle = \sqrt{p} |0\rangle + \sqrt{1-p} |1\rangle \quad (8)$$

with a real number  $p$  ( $0 \leq p \leq 1$ ). Here the vectors  $\{|0\rangle, |1\rangle\}$  are eigenstates of  $\sigma_z$  such that  $\sigma_z |0\rangle = |0\rangle$  and  $\sigma_z |1\rangle = -|1\rangle$ , where  $\sigma_{x,y,z}$  are conventional Pauli

matrices. We take a unitary operator

$$U = I \otimes |0\rangle\langle 0| + \sigma_z \otimes |1\rangle\langle 1| = \begin{pmatrix} 1 & 0 & 0 & 0 \\ 0 & 1 & 0 & 0 \\ 0 & 0 & 1 & 0 \\ 0 & 0 & 0 & -1 \end{pmatrix} \quad (9)$$

which acts on  $\mathbb{C}^2 \otimes \mathbb{C}^2$ , where  $I$  is the two-dimensional identity matrix. By substituting them into Eq. (2) we obtain a channel

$$\mathcal{E}(\rho_s) = \text{Tr}_e \left( U \rho_s \otimes |\psi_e\rangle\langle\psi_e| U^\dagger \right) = E_0 \rho_s E_0^\dagger + E_1 \rho_s E_1^\dagger \quad (10)$$

with

$$E_0 = \langle 0|U|\psi_e\rangle = \sqrt{p} I, \quad (11)$$

$$E_1 = \langle 1|U|\psi_e\rangle = \sqrt{1-p} \sigma_z. \quad (12)$$

Any initial state of a one-qubit system is parametrized as

$$\rho_s = \begin{pmatrix} \rho_{00} & \rho_{01} \\ \rho_{10} & \rho_{11} \end{pmatrix} = \frac{1}{2}(I + a_x \sigma_x + a_y \sigma_y + a_z \sigma_z) \quad (13)$$

with real numbers  $a_x, a_y, a_z$  such that  $a_x^2 + a_y^2 + a_z^2 \leq 1$ . The vector  $(a_x, a_y, a_z)$  is called the Bloch vector. The angle  $\phi$  defined by

$$2\rho_{10} = a_x + ia_y = e^{i\phi} \sqrt{a_x^2 + a_y^2} \quad (14)$$

denotes the azimuthal angle of the Bloch vector, and is called the phase of the spin. The quantity  $a_x + ia_y$  is called an amplitude in the context of NMR. The channel (10) transforms  $\rho_s$  to

$$\begin{aligned} \mathcal{E}(\rho_s) &= \frac{1}{2}p(I + a_x \sigma_x + a_y \sigma_y + a_z \sigma_z) \\ &\quad + \frac{1}{2}(1-p)(I - a_x \sigma_x - a_y \sigma_y + a_z \sigma_z) \\ &= \begin{pmatrix} \rho_{00} & (2p-1)\rho_{01} \\ (2p-1)\rho_{10} & \rho_{11} \end{pmatrix}. \end{aligned} \quad (15)$$

The first expression in the right hand side shows that the phase is left unchanged with probability  $p$  while it is flipped as  $e^{i\phi} \rightarrow e^{i(\phi+\pi)} = -e^{i\phi}$  with probability  $1-p$ . Hence it is natural to call this a phase flip channel. In particular, when  $p = \frac{1}{2}$ , the transverse components  $(a_x, a_y)$  of the Bloch vector, or the off-diagonal elements  $\rho_{01} = \rho_{10}^*$ , vanish after the channel is applied and the information about the phase is completely lost. However, the diagonal elements  $\rho_{00}$  and  $\rho_{11}$ , which represent population of the states  $|0\rangle$  and  $|1\rangle$ , remain unchanged. Due to these properties, the decoherence generated via the phase flip channel is called phase decoherence.

It should be noted that different sets of an initial state of the environment and a unitary operator of the whole system may yield the same channel. Instead of Eq. (8) and (9), we may take a mixed environment state

$$\rho_e = p|+\rangle\langle+| + (1-p)|-\rangle\langle-| = \frac{1}{2} \begin{pmatrix} 1 & 2p-1 \\ 2p-1 & 1 \end{pmatrix}, \quad (16)$$

where  $|+\rangle$  and  $|-\rangle$  are the normalized eigenvectors of  $\sigma_x$  with the eigenvalues 1 and  $-1$  respectively, and the controlled NOT gate

$$U_{\text{CNOT}} = \begin{pmatrix} 1 & 0 & 0 & 0 \\ 0 & 1 & 0 & 0 \\ 0 & 0 & 0 & 1 \\ 0 & 0 & 1 & 0 \end{pmatrix} = I \otimes |+\rangle\langle+| + \sigma_z \otimes |-\rangle\langle-|. \quad (17)$$

Substituting them into Eq. (2) we obtain again the phase flip channel Eq. (15).

## B. Random fluctuating field

It is possible to reproduce the phase flip channel without resort to the partial trace. This is done by introducing the mixing process defined below.

Let us consider a single spin Hamiltonian

$$H_{\text{rf}} = -\omega(t) \frac{\sigma_z}{2}, \quad (18)$$

where  $\omega(t)$  is a randomly fluctuating field. We have taken the natural unit  $\hbar = 1$ . Let us define the phase shift gate

$$S(\theta) = e^{i\theta\sigma_z/2} \quad (19)$$

with

$$\theta = \int_0^t \omega(\tau) d\tau. \quad (20)$$

The phase  $\theta$  integrates the effect of  $\omega(t)$  in the interval  $[0, t]$ . In the context of NMR, the phase shift gate is implemented with a longitudinal magnetic field or a scalar coupling with another spins as we discuss later. The phase shift gate acts on a density matrix as

$$S(\theta)\rho_s S^\dagger(\theta) = \begin{pmatrix} \rho_{00} & e^{i\theta}\rho_{01} \\ e^{-i\theta}\rho_{10} & \rho_{11} \end{pmatrix}. \quad (21)$$

Given a probability distribution  $p(\theta)$ , or the characteristic of the random fluctuating field, the mixing process is calculated as

$$\mathcal{M}(\rho_s) = \int_{-\infty}^{\infty} p(\theta) S(\theta) \rho_s S^\dagger(\theta) d\theta = \begin{pmatrix} \rho_{00} & \langle e^{i\theta} \rangle \rho_{01} \\ \langle e^{-i\theta} \rangle \rho_{10} & \rho_{11} \end{pmatrix}, \quad (22)$$

as given in [13]. For any probability distribution  $p(\theta)$ ,

$$\left| \langle e^{-i\theta} \rangle \right| = \left| \int_{-\infty}^{\infty} p(\theta) e^{-i\theta} d\theta \right| \leq \int_{-\infty}^{\infty} |p(\theta) e^{-i\theta}| d\theta = 1.$$

Hence, the absolute value of the off-diagonal elements of  $\mathcal{M}(\rho_s)$  become smaller than those of  $\rho_s$ . When the average  $\langle e^{-i\theta} \rangle$  is a real number, the map  $\mathcal{M}(\rho_s)$  reproduces the phase flip channel (15). This applies when  $p(\theta) = p(-\theta)$  for example.

We can further simplify the model without losing the essence of random fluctuating field model. Suppose  $\omega(t)$  assumes only two values,  $\omega_0 \pm \delta\omega$ , with the corresponding probabilities  $p(\pm\delta\omega)$ . We simulate phase decoherence phenomena according to this simplified random fluctuating field model.

For nuclear spin qubits, relaxation phenomena, including phase decoherence, have long been studied in somewhat different context in non-equilibrium statistical physics and employed as probes in condensed matter physics [14]. Studies on a relaxation process induced by environmental fluctuations have played an essential role when we want to extract information on the environments. Conversely, we can evaluate the time evolution of a system provided that the structure of the environment as well as the interaction between the system and the environment are given. Spin relaxation has often been analyzed by the phenomenological Bloch equations. The equations are characterized by two parameters called the longitudinal relaxation time  $T_1$  and the transverse relaxation time  $T_2$ . The former characterizes energy relaxation whereas the latter describes phase decoherence. Relaxation phenomena can also be described by the method of master equation: This is called a Redfield equation in the field of spin relaxation. Both the Bloch and the Redfield equations are valid only for the so-called narrowing limit where the characteristic time  $\tau_e$  of the environment is very short resulting in an exponential decay in the relevant spin variables. In contrast, the random fluctuating field model, though phenomenological, is applicable to any time scale ranging from the narrowing limit ( $\tau_e \rightarrow 0$ ) to the slow modulation with large  $\tau_e$ . Therefore, it is reasonable to take the random fluctuating field model as a basis for simulating phase decoherence phenomena.

### C. Suppressing decoherence by the bang-bang control

Several groups [7, 8] have proposed and analyzed a useful technique to suppress decoherence, which is called a quantum bang-bang control. We briefly explain the principle of the bang-bang control. When a qubit system evolves in time, the interaction with its environment usually causes decoherence in the qubit state. If, however, time-evolution of the qubit could be reversed by some methods, the qubit returns to its initial state and decoherence would be eliminated. Concerning the phase decoherence, a time-reversal operation can be simply implemented with a pair of  $\pi$ -pulses assuming that the state of environment remains unchanged between two pulses. The  $\pi$ -pulses around the  $x$  and  $-x$ -axis transform the qubit state with unitary operators

$$V = e^{-i\pi\sigma_x/2}, \quad V^\dagger = e^{i\pi\sigma_x/2}. \quad (23)$$

The phase shift operator  $S(\theta) = e^{i\theta\sigma_z/2}$  has the property

$$V^\dagger S(\theta)V = S(-\theta) = S(\theta)^{-1}. \quad (24)$$

Hence, by inserting a pair of  $\pi$ -pulses in a product of phase shift operators  $S(\theta)$  we get

$$V^\dagger S(\theta)VS(\theta) = I. \quad (25)$$

Therefore, the state  $\rho_s$  of the qubit comes back to the initial one as

$$(V^\dagger S(\theta)VS(\theta))\rho_s(V^\dagger S(\theta)VS(\theta))^\dagger = \rho_s. \quad (26)$$

The phase shift is also canceled if a pair of  $\pi$ -pulses is inserted as

$$S(\theta_2)V^\dagger S(\theta_2 + \theta_1)VS(\theta_1) = I \quad (27)$$

showing that the locations of  $\pi$ -pulse insertions may be chosen rather arbitrarily.

If the interaction with environment causes a phase shift proportional to time, a time-evolution operator  $S(\omega t)$  affects the qubit state. Here  $\omega$  is a parameter which characterizes the environment state and strength of interaction between the system and the environment. Let us introduce a time interval  $t_b$  and put  $2nt_b = t$  with a positive integer  $n$ . Then we have

$$\underbrace{S(\omega t_b) \cdot S(\omega t_b) \cdots S(\omega t_b) \cdot S(\omega t_b)}_{2n} = S(\omega t). \quad (28)$$

By inserting  $\pi$ -pulses we recover the initial state as

$$V^\dagger S(\omega t_b)VS(\omega t_b) \cdots V^\dagger S(\omega t_b)VS(\omega t_b) = I. \quad (29)$$

This argument indicates that phase decoherence is suppressed by applying a regular sequence of  $\pi$ -pulses on the qubit.

In a general circumstance, the environment state is not stationary and the phase shift is not proportional to time. Then  $S(\omega t)$  is replaced with

$$U(t; t_0) = S \left( \int_{t_0}^t \omega(\tau) d\tau \right). \quad (30)$$

Even in such a general case, if  $\omega(t)$  dose not vary rapidly and remains almost constant during the short time interval  $t_b$ , it is legitimate to use approximation

$$U(t_0 + 2t_b; t_0 + t_b) \approx U(t_0 + t_b; t_0) \quad (31)$$

and hence

$$V^\dagger U(t_0 + 2t_b; t_0 + t_b) V U(t_0 + t_b; t_0) \approx I. \quad (32)$$

Therefore, by inserting  $\pi$ -pulses with a short interval  $t_b$  in the time-evolution (30), the phase shift will be mostly canceled, and hence the associated decoherence will be suppressed.

## IV. TWO-QUBIT SYSTEM AS A COMPOSITE OF SYSTEM AND ENVIRONMENT

### A. Artificial environment

Any system in an environment has a Hamiltonian of the form

$$H_t = H_s + H_e + H_{se}, \quad (33)$$

where  $H_s$  and  $H_e$  govern intrinsic behaviors of the system and the environment, respectively, while  $H_{se}$  describes the interaction between them. Decomposition of the Hamiltonian in this manner is schematically depicted in Fig. 1. Zurek [15], for example, discussed a simple model where a one-qubit system is coupled to an  $n$ -qubit environment through interaction of the form  $\sigma_z \otimes \sigma_z$ .

Suppose the interaction  $H_{se}$  is so weak that the effect of  $H_{se}$  is negligible compared with that of  $H_s$  for a certain time scale  $\tau$ . Assume further that the system consists of two subsystems, which are referred to as subsystems 1 and 2. Then the system Hamiltonian  $H_s$  is decomposed as

$$H_s = H_1 + H_2 + H_{12}. \quad (34)$$

Here  $H_1$  and  $H_2$  control intrinsic behaviors of the subsystems, while  $H_{12}$  denotes interaction between them. Under this decomposition, we may regard the subsystem 1 as a new system and the subsystem 2 as an artificial environment. Then the subsystem 1 will exhibit a decoherence-like behavior if the subsystem 2 simulates an environment that has many degrees of freedom.

Particularly, nuclear spins used in NMR have long relaxation times of the order of  $\tau \sim 10$  s. Thus nuclear spins are almost isolated from the environment in the time scale  $\tau$ . In such a circumstance it is legitimate to regard some of the spins as an artificial environment for the other spins.

Zhang *et al.* [16] experimentally studied the spin dynamics of  $^{13}\text{C}$ -labeled trichloroethane, which has three spins in a molecule. They regarded three spins as a composite of a two-qubit system and a one-qubit environment. They claimed that they observed decoherence in

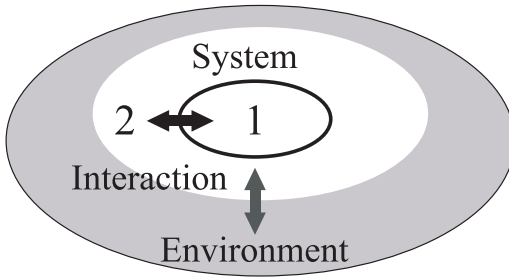


FIG. 1: A system and an environment. The system consists of two subsystems, 1 and 2.

the two-qubit system. However, the artificial environment must have a large number of degrees of freedom to induce irreversible decoherence-like behavior in the system while the one-qubit environment employed in their experiments had not enough degrees of freedom. Hence their system exhibited a periodic behavior and failed to introduce an irreversible change in the system.

Teklemariam *et al.* [17] proposed to apply a stochastic classical field [18] on the artificial environment to generate artificial decoherence. Although the artificial environment has only a few degrees of freedom, it can simulate an open environment if it is randomized by an external stochastic field. With this idea, they observed decoherence-like behavior by using NMR.

Although we closely follow Teklemariam *et al.*, we simplify the principle for generating artificial phase decoherence phenomena to the limit. Thanks to this simplification, we are able to analyze the phenomena without numerical calculations and compare theoretical and experimental results directly. Moreover, we test the bang-bang control for suppressing decoherence. These new results will be explained in the following.

### B. Two-qubit system

In the rest of this paper we shall study a two-qubit system. Each qubit is referred to as qubit 1 and qubit 2, respectively. Qubit 1 is regarded as a system while qubit 2 as an environment coupled to qubit 1. We will use terminology of NMR for experimental applications. The spin operators of a nucleus are denoted as  $I_k = \sigma_k/2$  ( $k = x, y, z$ ). A static uniform magnetic field  $B_0$  is applied to the two-qubit system. The Hamiltonian of the whole system is

$$H = -\omega_{0,1}I_z \otimes I - \omega_{0,2}I \otimes I_z + JI_z \otimes I_z, \quad (35)$$

where  $\omega_{0,i} = \gamma_i B_0$ ,  $\gamma_i$  being the gyromagnetic ratio of the nucleus  $i$ , and  $J$  is a scalar coupling constant between the spins. Although the sign of  $J$  is irrelevant to our arguments, we assume  $J > 0$  for definiteness. The state of the whole system evolves following the Schrödinger equation  $i\frac{d}{dt}|\psi(t)\rangle = H|\psi(t)\rangle$ . If we apply a time-dependent unitary transformation

$$R = e^{-i(\omega_{0,1}-J/2)I_z t} \otimes e^{-i\omega_{0,2}I_z t} \quad (36)$$

on the state of the two-qubit system as  $|\tilde{\psi}(t)\rangle = R|\psi(t)\rangle$ , we get

$$\begin{aligned} i\frac{d}{dt}|\tilde{\psi}(t)\rangle &= iR\frac{d}{dt}|\psi(t)\rangle + i\frac{dR}{dt}|\psi(t)\rangle \\ &= RH|\psi(t)\rangle + i\frac{dR}{dt}|\psi(t)\rangle \\ &= RHR^\dagger|\tilde{\psi}(t)\rangle + i\frac{dR}{dt}R^\dagger|\tilde{\psi}(t)\rangle. \end{aligned}$$

Therefore, the transformed state  $|\tilde{\psi}(t)\rangle$  satisfies the Schrödinger equation  $i\frac{d}{dt}|\tilde{\psi}(t)\rangle = \tilde{H}|\tilde{\psi}(t)\rangle$  with the trans-

formed Hamiltonian

$$\tilde{H} = RHR^\dagger + i\frac{dR}{dt}R^\dagger = JI_z \otimes \left(I_z - \frac{1}{2}I\right). \quad (37)$$

The time-dependent operator (36) transforms a coordinate system from the laboratory frame to a rotating frame.

When the Hamiltonian (37) acts on states  $|\tilde{\psi}\rangle \otimes |\tilde{0}\rangle$  and  $|\tilde{\psi}\rangle \otimes |\tilde{1}\rangle$ , it yields

$$\tilde{H}|\tilde{\psi}\rangle \otimes |\tilde{0}\rangle = 0, \quad (38)$$

$$\tilde{H}|\tilde{\psi}\rangle \otimes |\tilde{1}\rangle = (-JI_z|\tilde{\psi}\rangle) \otimes |\tilde{1}\rangle, \quad (39)$$

respectively. Thus the Hamiltonian  $\tilde{H}$  describes an effective magnetic field acting on qubit 1. The effective magnetic field is switched on when qubit 2 is in the state  $|\tilde{1}\rangle$  and it is switched off when qubit 2 is in  $|\tilde{0}\rangle$ . Hence, by manipulating qubit 2, we can realize a fluctuating environment for qubit 1. We will extensively use this fact in the following. We will be concerned with the rotating system defined by Eq. (36) in the following and the symbol  $\sim$  will be omitted henceforth to simplify the notations.

In the next two subsections, we show two examples of artificially generated phase decoherence phenomena: One is phase decoherence of a single qubit in a transmission line, and the other is that in a quantum memory. The difference between these two examples is that of the characteristic of the random fields. We emphasize that any phase decoherence phenomena can be generated by selecting a proper random fluctuating field.

### C. Phase decoherence in a quantum transmission line and its suppression by the bang-bang control

Let us imagine a situation such that a flying qubit passes through a quantum transmission line and a noise hits the qubit in the line. The noise source is assumed to localize at a certain position in the line [19].

We construct a model which realizes the above situation with the two-qubit system discussed in the previous section. We regard qubit 1 as a flying qubit and qubit 2 as an environment. Suppose that the initial state of qubit 2 is  $|0\rangle$ . At time  $t_1$ , which corresponds to the noise position in the transmission line, we flip qubit 2 to  $|1\rangle$  and at time  $t_1 + \Delta$  we flip it back to  $|0\rangle$ . We then observe qubit 1 at later time  $T$  ( $> t_1 + \Delta$ ). Qubit 1 at  $T$  is transformed by the phase shift

$$e^{-i\int_0^T \tilde{H}(t)dt} = e^{iJI_z\Delta} = S(J\Delta). \quad (40)$$

Now we regard the time interval  $\Delta$  as a random variable. Assume that  $\Delta$  takes its value in the range  $0 \leq J\Delta \leq 2\pi$  with uniform probability distribution. Then the mixing process (22) yields

$$\mathcal{M}(\rho_s) = \frac{1}{2\pi} \int_0^{2\pi} S(\theta)\rho_s S^\dagger(\theta)d\theta = \begin{pmatrix} \rho_{00} & 0 \\ 0 & \rho_{11} \end{pmatrix}. \quad (41)$$

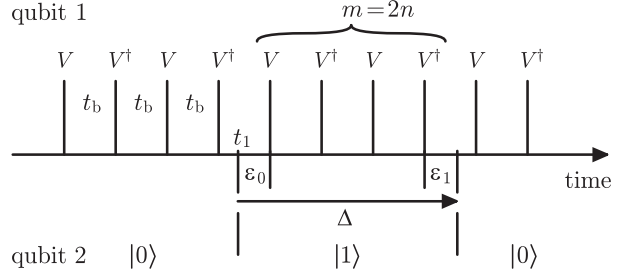


FIG. 2: The bang-bang pulses,  $V$  and  $V^\dagger$ , are applied on qubit 1. Qubit 2 is flipped to  $|1\rangle$  at  $t_1$  and is flipped back to  $|0\rangle$  at  $t_1 + \Delta$ . This depicts the case (1),  $U_1$  of Eq. (43).

Thus, a complete decoherence takes place in qubit 1.

Let us apply the bang-bang control to qubit 1 in the artificial phase flip channel discussed above. Assume that the initial state of qubit 2 is  $|0\rangle$ . Apply  $\pi$ -pulse sequence,  $V$  and  $V^\dagger$  of (23), with constant time interval  $t_b$  on qubit 1 during  $0 \leq t \leq T$ . At time  $t_1$  qubit 2 turns to  $|1\rangle$  and at time  $t_1 + \Delta$  it turns back to  $|0\rangle$ . The time  $t_1$  and the interval  $\Delta$  are random variables. The value of  $\Delta$  varies in the range  $0 \leq J\Delta \leq 2\pi$  with uniform probability distribution. Measure qubit 1 state at time  $T$  and take an average of the data with respect to the random variables  $t_1$  and  $\Delta$ . What is the resulting state  $\mathcal{M}(\rho_s)$  for this mixing process?

We consider four cases separately:

- (1) there are even number of  $\pi$ -pulses in  $[0, t_1]$  and even number of  $\pi$ -pulses in  $[t_1, t_1 + \Delta]$ ;
- (2) even in  $[0, t_1]$  and odd in  $[t_1, t_1 + \Delta]$ ;
- (3) odd in  $[0, t_1]$  and even in  $[t_1, t_1 + \Delta]$ ;
- (4) odd in  $[0, t_1]$  and odd in  $[t_1, t_1 + \Delta]$ .

Define  $\varepsilon_0$  such that the first  $\pi$ -pulse in  $t_1 \leq t \leq t_1 + \Delta$  is applied at  $t = t_1 + \varepsilon_0$ . Similarly, define  $\varepsilon_1$  such that the final  $\pi$ -pulse in  $t_1 \leq t \leq t_1 + \Delta$  is applied at  $t = t_1 + \Delta - \varepsilon_1$ . If the number of  $\pi$ -pulses in  $t_1 \leq t \leq t_1 + \Delta$  is  $m$ ,

$$\Delta = \varepsilon_0 + (m - 1)t_b + \varepsilon_1. \quad (42)$$

Assume that  $Jt_b \ll 2\pi$  so that there are sufficiently many pulses in the interval  $[t_1, t_1 + \Delta]$ . This assumption is justified for a real nuclear spins. Under this assumption, the variables  $\varepsilon_0$  and  $\varepsilon_1$  are regarded as random variables taking values in the range  $0 \leq \varepsilon_i \leq t_b$  with uniform probability distribution.

The time-evolution operator for qubit 1 is calculated for each case as follows. We put  $L(\Delta) = S(J\Delta)$ . The sequence of  $\pi$ -pulse pairs is represented by alternate insertions of  $V$  and  $V^\dagger$  of Eq. (23) in the time-evolution operator product. For the case (1), the number of  $\pi$ -pulses is  $m = 2n$ . The time-evolution operator is calculated

with a help of Fig. 2 as

$$\begin{aligned}
U_1 &= L(\varepsilon_1)V^\dagger L(t_b)V \left[ L(t_b)V^\dagger L(t_b)V \right]^{n-1} L(\varepsilon_0) \\
&= L(\varepsilon_1)V^\dagger L(t_b)V L(\varepsilon_0) \\
&= L(\varepsilon_1)L(-t_b)L(\varepsilon_0) \\
&= L(\varepsilon_1 - t_b + \varepsilon_0),
\end{aligned} \tag{43}$$

where use has been made of the property of  $V$ , Eq. (24). For the case (2) with  $m = 2n + 1$ , we obtain

$$\begin{aligned}
U_2 &= V^\dagger L(\varepsilon_1)V \left[ L(t_b)V^\dagger L(t_b)V \right]^n L(\varepsilon_0) \\
&= V^\dagger L(\varepsilon_1)V L(\varepsilon_0) \\
&= L(-\varepsilon_1)L(\varepsilon_0) \\
&= L(-\varepsilon_1 + \varepsilon_0).
\end{aligned} \tag{44}$$

For the case (3) with  $m = 2n$ ,

$$\begin{aligned}
U_3 &= V^\dagger L(\varepsilon_1)V L(t_b)V^\dagger \left[ L(t_b)V L(t_b)V^\dagger \right]^{n-1} L(\varepsilon_0)V \\
&= V^\dagger L(\varepsilon_1)V L(t_b)V^\dagger L(\varepsilon_0)V \\
&= V^\dagger L(\varepsilon_1)L(-t_b)L(\varepsilon_0)V \\
&= L(-\varepsilon_1 + t_b - \varepsilon_0).
\end{aligned} \tag{45}$$

Finally for the case (4) with  $m = 2n + 1$ ,

$$\begin{aligned}
U_4 &= L(\varepsilon_1)V^\dagger \left[ L(t_b)V L(t_b)V^\dagger \right]^n L(\varepsilon_0)V \\
&= L(\varepsilon_1)V^\dagger L(\varepsilon_0)V \\
&= L(\varepsilon_1 - \varepsilon_0).
\end{aligned} \tag{46}$$

By taking average with respect to  $\varepsilon_0$  and  $\varepsilon_1$ , and also average over the four cases, the mixing process (5) yields

$$\mathcal{M}(\rho_s) = \frac{1}{4} \frac{1}{t_b^2} \int_0^{t_b} d\varepsilon_0 \int_0^{t_b} d\varepsilon_1 \left( U_1 \rho_s U_1^\dagger + U_2 \rho_s U_2^\dagger + U_3 \rho_s U_3^\dagger + U_4 \rho_s U_4^\dagger \right). \tag{47}$$

Each term in the parentheses is calculated as;

$$\begin{aligned}
L(\varepsilon) \rho_s L^\dagger(\varepsilon) &= S(J\varepsilon) \rho_s S^\dagger(J\varepsilon) \\
&= \begin{pmatrix} \rho_{00} & e^{iJ\varepsilon} \rho_{01} \\ e^{-iJ\varepsilon} \rho_{10} & \rho_{11} \end{pmatrix}
\end{aligned} \tag{48}$$

while the integral is evaluated as

$$\frac{1}{t_b} \int_0^{t_b} d\varepsilon e^{iJ\varepsilon} = \frac{e^{iJt_b} - 1}{iJt_b} = \frac{\sin(Jt_b/2)}{Jt_b/2} e^{iJt_b/2}. \tag{49}$$

By combining these results we finally obtain

$$\mathcal{M}(\rho_s) = \begin{pmatrix} \rho_{00} & \kappa \rho_{01} \\ \kappa \rho_{10} & \rho_{11} \end{pmatrix}, \tag{50}$$

$$\kappa = \left\{ \frac{\sin(Jt_b/2)}{Jt_b/2} \right\}^2. \tag{51}$$

Comparing this result (50) with (41), we see that the bang-bang control suppresses phase decoherence. In particular, by making the interval of the bang-bang pulses infinitesimally short,  $t_b \rightarrow 0$ , we get  $\kappa \rightarrow 1$ , so the decoherence is removed and the initial state is completely preserved.

#### D. Phase decoherence in a quantum memory and its suppression by the bang-bang control

Suppose a qubit sits in a quantum memory device (quantum register). The qubit is exposed to a noisy environment and loses its phase coherence. The noise is described by the random fluctuating field in the Hamiltonian (18). We assume that the field variable  $\omega(t)$  in (18) has a white noise spectrum. This can also be interpreted as a model of the phase relaxation process in NMR [20]. The phase  $\theta$  of the qubit evolves in time and is randomly distributed at a later time. The distribution function  $p(\theta)$  of  $\theta$  is Gaussian,

$$p(\theta) = \frac{1}{\sqrt{2\pi}s} e^{-\theta^2/2s^2}, \tag{52}$$

where  $s^2$  is proportional to the evolution time  $t$  [20].

We can also construct a model which realizes the above situation with the previous two-qubit system by modifying the random field. We regard qubit 1 as a qubit registered in the memory and qubit 2 as an environment. Set the initial state of qubit 2 to  $|0\rangle$  at time  $t_0 = 0$ , turn it to  $|1\rangle$  at  $t_1$ , turn it back to  $|0\rangle$  at  $t_2$ , and repeat flipping qubit 2 at  $t_3, t_4$  and so on. Under this manipulation qubit 2 effectively works as a noisy environment for qubit 1. The time interval between consecutive flippings is denoted as

$$\Delta_j = t_{j+1} - t_j = \bar{\Delta}(1 + \alpha \xi_j) \quad (j = 0, 1, 2, \dots). \tag{53}$$

Here  $\{\xi_j\}$  are independent random variables following the probability distribution function

$$p(\xi_j) = \frac{1}{\sqrt{2\pi}} e^{-\xi_j^2/2}, \tag{54}$$

after (52).  $\bar{\Delta}$  is the average of  $\{\Delta_j\}$ . The parameter  $\alpha$  ( $0 \leq \alpha \leq 1/4$ ) characterizes variance of the time intervals. To ensure that  $\Delta_j$  in (53) is positive, the range of  $\xi_j$  should be  $-\frac{1}{\alpha} < \xi_j$ . However, if  $\alpha$  is not too large, the probability of having negative  $\Delta_j$  is negligibly small. Hence, it is legitimate to enlarge the range of  $\xi_j$  to  $-\infty < \xi_j < \infty$  when we take an average. At time  $t_{2n}$  the evolution operator for qubit 1 becomes

$$\begin{aligned}
U_\xi &= e^{-i \int_0^{t_{2n}} \tilde{H}(t) dt} \\
&= e^{i J I_z (\Delta_1 + \Delta_3 + \dots + \Delta_{2n-1})} \\
&= S(J(\Delta_1 + \Delta_3 + \dots + \Delta_{2n-1})). \tag{55}
\end{aligned}$$

In this case, the mixing process (5) yields

$$\begin{aligned}
\mathcal{M}(\rho_s) &= \int_{-\infty}^{\infty} d\xi_1 \int_{-\infty}^{\infty} d\xi_2 \dots \int_{-\infty}^{\infty} d\xi_{2n} \\
&\quad p(\xi_1) p(\xi_2) \dots p(\xi_{2n}) U_\xi \rho_s U_\xi^\dagger. \tag{56}
\end{aligned}$$

The matrix  $U_\xi \rho_s U_\xi^\dagger$  is calculated similarly to Eq. (48). The integral is evaluated as

$$\lambda = \int_{-\infty}^{\infty} d\xi p(\xi) e^{iJ\bar{\Delta}(1+\alpha\xi)} = e^{iJ\bar{\Delta}} e^{-\frac{1}{2}(J\bar{\Delta}\alpha)^2}. \tag{57}$$

Thus (56) becomes

$$\mathcal{M}(\rho_s) = \begin{pmatrix} \rho_{00} & \lambda^n \rho_{01} \\ (\lambda^*)^n \rho_{10} & \rho_{11} \end{pmatrix}, \quad (58)$$

at  $\overline{t_{2n}} = 2n\bar{\Delta}$ , the average of time  $t_{2n}$ . Then the absolute value of the matrix element  $\rho_{01}$  in  $\mathcal{M}(\rho_s)$  is multiplied by

$$\begin{aligned} |\lambda|^n &= \exp \left\{ -\frac{1}{2}(J\bar{\Delta}\alpha)^2 \frac{\overline{t_{2n}}}{2\bar{\Delta}} \right\} \\ &= \exp \left( -\frac{1}{4}J^2\alpha^2\bar{\Delta}\overline{t_{2n}} \right) = e^{-\overline{t_{2n}}/T_2^*}. \end{aligned} \quad (59)$$

The last line defines  $T_2^*$  which we call the effective transverse relaxation time, since  $\mathcal{M}(\rho_s)$  is calculated only at  $\overline{t_{2n}}$ . We note that  $\bar{\Delta}$  is regarded as the correlation time of the artificial environment and that the decay of  $|\rho_{01}|$  is non-exponential for  $t \sim \bar{\Delta}$ . Thus, we see that phase decoherence in the presence of random fluctuating field is characterized by the decay constant

$$T_2^* = \frac{4}{J^2\alpha^2\bar{\Delta}}. \quad (60)$$

It is clear that  $T_2^*$  becomes shorter for the larger variance  $\alpha$  of fluctuation of the effective magnetic field.

Now let us apply the bang-bang control along with the artificial random fluctuating field. Assume that the bang-bang pulse interval  $t_b$  is short enough so that  $t_b \ll \alpha\bar{\Delta}$  is satisfied. Then the argument of the previous subsection to evaluate  $\mathcal{M}(\rho_s)$  is applicable here as well. For  $\overline{t_{2n}} = 2n\bar{\Delta}$ , there are  $n$  times of random switch-on of qubit 2 on average. After one cycle of switching-on and -off of qubit 2, the element  $\rho_{01}$  of the density matrix is multiplied with the factor  $\kappa$  given by Eq. (51). Therefore the off-diagonal element  $\rho_{01}$  is multiplied by

$$\kappa^n = \kappa^{\overline{t_{2n}}/(2\bar{\Delta})} = e^{-\overline{t_{2n}}/T_{2b}^*} \quad (61)$$

at  $\overline{t_{2n}}$ . Eq. (61) defines  $T_{2b}^*$ , the decay constant that characterizes the phase decoherence under the bang-bang control. It is explicitly given as

$$T_{2b}^* = -\frac{2\bar{\Delta}}{\ln \kappa} = \bar{\Delta} \left\{ \ln \left| \frac{Jt_b/2}{\sin(Jt_b/2)} \right| \right\}^{-1}. \quad (62)$$

Note that  $\kappa \rightarrow 1$  and hence  $T_{2b}^* \rightarrow \infty$  as  $t_b \rightarrow 0$ . Therefore decoherence is perfectly eliminated by bang-bang pulses with infinitesimally short interval.

Here we would like to give a remark on the work by Teklemariam *et al.* [17]. They used a three-spin molecule as a composite of a one-qubit system and a two-qubit environment. Their initial state vector takes the form  $|\chi_s\rangle \otimes |\phi_e\rangle \otimes |\psi_e\rangle$ . Their Hamiltonian in our notation is

$$\begin{aligned} H &= -\omega_{0,1}I_z \otimes I \otimes I - \omega_{0,2}I \otimes I_z \otimes I \\ &\quad - \omega_{0,3}I \otimes I \otimes I_z + J_{12}I_z \otimes I_z \otimes I \\ &\quad + J_{13}I_z \otimes I \otimes I_z + J_{23}I \otimes I_z \otimes I_z, \end{aligned}$$

with which the time-evolution operator  $U(t) = e^{-iHt}$  is defined. They introduced a kick operator

$$K(\xi, \zeta) = I \otimes e^{i\xi\sigma_y} \otimes e^{i\zeta\sigma_y},$$

which acts on the artificial environment. Here  $\xi$  and  $\zeta$  are random variables, which are interpreted as kick angles. Now the time evolution operator of the whole system is

$$\begin{aligned} U_{\xi, \zeta} &= K(\xi_n, \zeta_n)U(t)K(\xi_{n-1}, \zeta_{n-1})U(t) \cdots \\ &\quad \cdots K(\xi_2, \zeta_2)U(t)K(\xi_1, \zeta_1)U(t). \end{aligned}$$

This should be compared with our time-evolution operator (55). Their strategy to manipulate the environment is different from ours. A channel associated with their model is defined if  $U_{\xi, \zeta}$  is substituting into (2). A two-qubit environment is required to simulate an arbitrary one-qubit channel. In contrast, we are interested in this paper only in the phase decoherence and a one-qubit environment is sufficient for this purpose as discussed above.

## V. EXPERIMENTS

We demonstrate generation and suppression of phase decoherence experimentally with an NMR quantum computer. A 0.6 ml, 200 mM sample of  $^{13}\text{C}$ -labeled chloroform (Cambridge Isotope) in d-6 acetone is employed as a two-qubit molecule. The spin of carbon nucleus in chloroform is referred to as spin 1 (qubit 1), while the spin of hydrogen nucleus is referred to as spin 2 (qubit 2). Data is taken at room temperature with a JEOL ECA-500 NMR spectrometer [21], whose hydrogen Larmor frequency is approximately 500 MHz. The measured spin-spin coupling constant is  $J/2\pi = 215.5$  Hz. The transverse relaxation times in a natural environment are  $T_2 \sim 0.30$  s for the carbon nucleus and  $T_2 \sim 7.5$  s for the hydrogen nucleus. The longitudinal relaxation times are measured to be  $T_1 \sim 20$  s for both nuclei. The duration of a  $\pi$ -pulse for both nuclei is set to 50  $\mu\text{s}$ . Precision of pulse duration control is 100 ns.

### A. Demonstration of the phase decoherence in a quantum transmission line

The model of the phase decoherence in a transmission line is implemented in NMR. The scheme of the experiment is shown in Fig. 3. Time evolution of spins is depicted in Fig. 3 (a) in terms of the Bloch vectors viewed in the rotating frame defined in terms of the transformation (36). Both spins are set initially in the state  $|0\rangle$ . This initial state is prepared as a so-called pseudopure state [22]. To begin with spin 1 is turned by a  $\pi/2$ -pulse at  $t = 0$ . Spin 2 is flipped by a  $\pi$ -pulse at  $t = t_1$  and then flipped back to  $|0\rangle$  by another  $\pi$ -pulse at  $t = t_1 + \Delta$ . Spin 1 evolves according to the Hamiltonians (38) and (39). Spin 1 remains stationary while spin 2 is in the state  $|0\rangle$ . Spin 1 precesses with the angular velocity  $J$

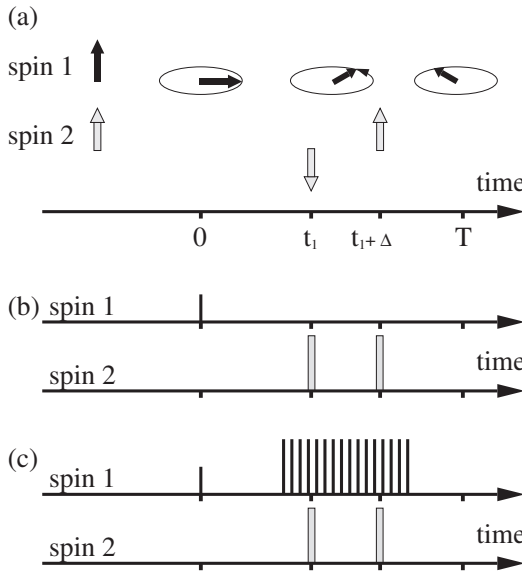


FIG. 3: The experimental scheme of phase decoherence of a qubit in a transmission line. (a) Motion of the spin Bloch vectors viewed in the rotating frame. (b) The pulse sequence for implementing the phase flip channel. The short bar denotes a  $\pi/2$ -pulse while the long bar denotes a  $\pi$ -pulse. (c) The pulse sequence for the bang-bang control. A regular sequence of  $\pi$ -pulses with a constant interval  $t_b$  is applied on spin 1.

while spin 2 is in the state  $|1\rangle$ . The state of spin 1 at  $t = T$  is measured via a free induction decay (FID) signal. Figure 3 (b) is a schematic picture of the pulse sequence to manipulate these spins. The short bar corresponds to a  $\pi/2$ -pulse while the long bar to a  $\pi$ -pulse.

The measured quantities via FID signals are the components  $(a_x, a_y)$  of the Bloch vector of spin 1, which correspond to the off-diagonal elements of the density matrix (13). The complex amplitudes  $\{a_x + ia_y = e^{i\phi} \sqrt{a_x^2 + a_y^2}\}$  are plotted in Fig. 4. The measurements are repeated with variety of spin 2 inversion time  $\Delta$  uniformly distributed in the range  $[0, 2\pi/J] = [0, 1/215.5]$  s. The total number of repetition is 128 in our experiment.

The open squares  $\square$  in Fig. 4 show the measured amplitudes, where only 8 out of 128 amplitudes are shown. Their absolute values are close to unity while their phases are distributed in the range  $[0, 2\pi]$  due to the variation of spin 2 inversion time  $\Delta$ .

To construct a mixing process we take average of measured amplitudes. Each open triangle  $\triangle$  in Fig. 4 is an average of 16 amplitudes. There are  $8 = 128/16$  open triangles in total. It is found that the absolute values of the averaged amplitudes  $\triangle$  become considerably smaller than unity.

The open circle  $\circ$  in Fig. 4 shows the average of all 128 measured amplitudes. The averaged amplitude is close to the origin, which implies vanishing off-diagonal elements of the density matrix of spin 1 and therefore is a clear

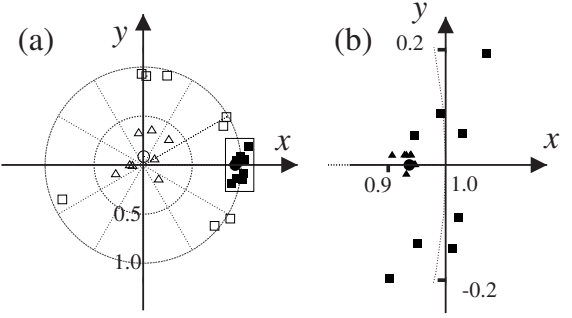


FIG. 4: Amplitude of spin 1 measured in the presence of phase decoherence in a transmission line (open symbols) and the same with the bang-bang control (filled symbols).  $\square, \blacksquare$ : individual amplitude measured via FID signals.  $\triangle, \blacktriangle$ : amplitude averaged over 16 measurements.  $\circ, \bullet$ : amplitude averaged over 128 measurements ( $16 \times 8 = 128$ ). The area surrounded by the rectangle in (a) is magnified in the panel (b).

indication of phase decoherence. Thus we see that this system works as an artificial phase flip channel for spin 1.

Next, we apply the bang-bang control to the system qubit. Figure 3 (c) shows the pulse sequence to implement the phase flip channel and the bang-bang control. We apply a regular series of  $\pi$ -pulses on spin 1 with the interval  $t_b = 0.3$  ms. The number of  $\pi$ -pulses is 16 in each run. The duration of  $\pi$ -pulses covers the period for which spin 2 is inverted. The rotation axes of the  $\pi$ -pulses for spin 1 are cyclically permuted as

$$(x, -x, y, -y, -x, x, -y, y) \quad (63)$$

in order to reduce influence of possible pulse imperfections. We repeat this procedure 128 times as spin 2 inversion time  $\Delta$  is varied.

The FID amplitudes in the presence of the bang-bang pulses are indicated as filled squares  $\blacksquare$  in Fig. 4. The panel (b) in Fig. 4 is a magnification of a part of the panel (a). The absolute values of these amplitudes are almost one. Moreover, their phases are concentrated in a narrow range,  $|\phi| \leq 0.25$  rad. This is comparable to the theoretical estimate  $Jt_b = 2\pi \times 215.5 \times 0.3 \times 10^{-3} \simeq 0.4$  rad.

The filled triangle  $\blacktriangle$  in Fig. 4 is an average of 16 amplitudes in the presence of the bang-bang control. The filled circle  $\bullet$  in Fig. 4 is the average of 128 amplitudes. The average of the whole data is  $0.93 + 0.0i \pm 0.1i$ . The error in the  $y$ -component originates from the FID phase determination error. This magnitude 0.93 should be compared with the theoretical prediction  $\kappa = 0.986$  from Eq. (51). This shows that the bang-bang control suppresses phase decoherence as expected.

## B. Demonstration of the phase decoherence in a quantum memory

The model of the phase decoherence in a quantum memory is also implemented in NMR. We use the same two-spin molecule as in the previous experiment. Both spins are initially set to the up-state  $|0\rangle$ . Spin 1 is turned by a  $\pi/2$ -pulse at  $t = t_0 = 0$  while spin 2 is flipped from  $|0\rangle$  to  $|1\rangle$  by a  $\pi$ -pulse at  $t = t_{2k-1}$  and is flipped back from  $|1\rangle$  to  $|0\rangle$  by a subsequent  $\pi$ -pulse at  $t = t_{2k}$  ( $k = 1, 2, 3, \dots$ ). The time intervals  $\{\Delta_j = t_{j+1} - t_j\}$  between adjacent  $\pi$ -pulses distribute according to the Gaussian distribution (53) and (54). The spin 1 evolves obeying the Hamiltonians (38) and (39). Spin 1 remains stationary when spin 2 is in the state  $|0\rangle$  while it precesses when spin 2 is in  $|1\rangle$ . The state of spin 1 at  $t = T$  is measured via a FID signal. The magnitude of the measured amplitude,  $\sqrt{a_x^2 + a_y^2}$ , is plotted as a function of  $T$  in Fig. 6.

In the first run, depicted in Fig. 5 (a), we put  $\alpha = 0$  and hence the time interval between  $\pi$ -pulses is a constant taking value  $\Delta_j = \bar{\Delta} = 2.0$  ms. In this case a regular alternating field acts on spin 1. If the  $\pi$ -pulses and the spin dynamics were perfect, there would be no decoherence. However, in reality, it is impossible to avoid pulse imperfection, measurement errors and intrinsic decoherence. Figure 6 shows that decoherence takes place even in the system under regular pulses. The measurement with  $\alpha = 0$  is necessary as a reference to the other measurements with  $\alpha \neq 0$ . We may claim that decoherence is enhanced by the random fluctuating field if we observe faster decoherence in the measurement with  $\alpha \neq 0$  than that with  $\alpha = 0$ . The rotation axes of the  $\pi$ -pulses for spin 2 are chosen again as in Eq. (63) to reduce undesired influence of imperfection in the  $\pi$ -pulses. Thus the number of  $\pi$ -pulses are set to a multiple of 8. The magnitudes of measured amplitudes under the pulses with  $\alpha = 0$  are plotted as filled squares ■ in Fig. 6. The measured decoherence factor for  $\alpha = 0$  is

$$e^{-T/T_2^*} = 0.45 \quad \text{at } T = 100 \text{ ms.} \quad (64)$$

Next, we modulate randomly the time intervals of spin 2 flippings. The corresponding pulse sequence is shown in Fig. 5 (b). The variance of the intervals in Eq. (53) is chosen to be  $\alpha = 0.10, 0.15, 0.20$  and  $0.25$ . The average of the intervals is  $\bar{\Delta} = 2.0$  ms. A series of random variables  $\Xi = (\xi_0, \xi_1, \dots, \xi_r)$  is prepared according to the Gaussian distribution (54). Then a series of intervals  $(\Delta_0, \Delta_1, \dots, \Delta_r)$  is defined via (53) and then the amplitude  $a_x + ia_y$  of spin 1 is measured at time  $t = T$ . We prepare 128 series  $\{\Xi_1, \Xi_2, \dots, \Xi_{128}\}$ , repeat measurements 128 times and take an average of 128 measured amplitudes for each values of  $\alpha$  and  $T$ . The magnitude of the averaged amplitude is plotted as a function of  $T$  in Fig. 6. The correspondence between the symbol and the variance parameter  $\alpha$  is ( $\nabla$  :  $\alpha = 0.10$ ), ( $\triangle$  :  $\alpha = 0.15$ ), ( $\bigcirc$  :  $\alpha = 0.20$ ), ( $\square$  :  $\alpha = 0.25$ ). The

plotted data show exponential decrease in the magnitude of the amplitude  $a_x + ia_y$ . It is clearly seen that a larger variance  $\alpha$  causes faster decoherence in spin 1. The decoherence factors are read from the slopes of the graphs in Fig. 6 as

$$\begin{aligned} e^{-T/T_2^*} &= 0.31, 0.20, 0.10, 0.05 \quad \text{at } T = 100 \text{ ms} \\ \text{for } \alpha &= 0.10, 0.15, 0.20, 0.25. \end{aligned} \quad (65)$$

Let us introduce a dimensionless quantity

$$Q(\alpha) = -\frac{1}{\alpha^2} \ln \left\{ \frac{e^{-T/T_2^*}|_{\alpha \neq 0}}{e^{-T/T_2^*}|_{\alpha=0}} \right\} \quad (66)$$

to compare the measured data with the theoretical estimation. The theoretical prediction (59) yields

$$Q_{\text{theory}} = \frac{1}{4} J^2 \bar{\Delta} T = 92 \quad (67)$$

for  $J = 2\pi \times 215.5$  Hz,  $\bar{\Delta} = 2$  ms,  $T = 100$  ms, independently of  $\alpha$ . On the other hand, by substituting the measured values (64) and (65) into (66), we obtain

$$\begin{aligned} Q(\alpha) &= 37, 36, 38, 35 \\ \text{for } \alpha &= 0.10, 0.15, 0.20, 0.25. \end{aligned} \quad (68)$$

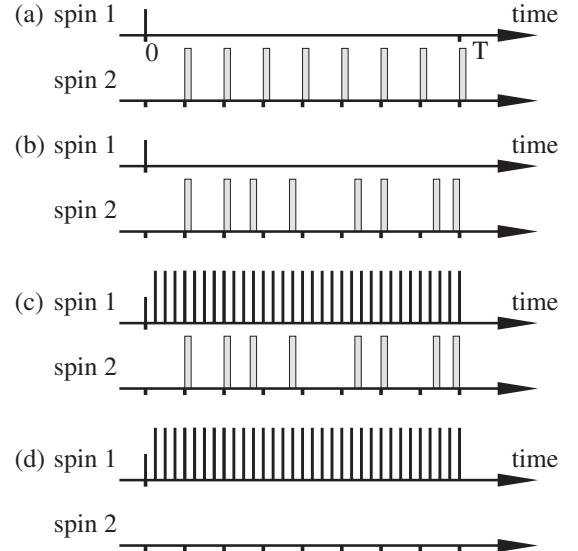


FIG. 5: The pulse sequences to implement the artificial phase decoherence in a quantum memory. The initial states of both spins are up-states. The short bar is a  $\pi/2$ -pulse and the long bar is a  $\pi$ -pulse. (a) A regular series of pulses with a fixed interval  $\bar{\Delta} = 2.0$  ms are applied on spin 2 as a reference to other experiments. (b) A series of pulses with random intervals are applied on spin 2. The variance of intervals is adjusted with the parameter  $\alpha$ . (c) The bang-bang control pulses are applied on spin 1 while random pulses are applied on spin 2. (d) The bang-bang pulses are applied on spin 1 while no pulses are applied on spin 2.

Thus, the theoretical estimates (67) do not agree quantitatively with the measured values (68). However, we observe that the value  $Q(\alpha)$  is almost independent of  $\alpha$ , implying that the decoherence rate  $(T_2^*)^{-1}$  is proportional to  $\alpha^2$  as predicted in (60).

It is observed in Fig. 6 that the data points deviate from the straight line in particular for the case with  $\alpha = 0.25$  with  $T \geq 80$  ms. We conducted a numerical simulation and found large fluctuation of averaged amplitudes in the region where the averaged amplitudes are small. This fluctuation comes from smallness of the statistical ensemble, whose size is 128 in our experiment.

Next, we apply the bang-bang control to spin 1. The pulse sequence to incorporate the bang-bang control is shown in Fig. 5 (c). A regular sequence of  $\pi$ -pulses with interval  $t_b$  is applied on spin 1. The rotation axes of these  $\pi$ -pulses are cyclically permuted as in Eq. (63). During this run, a sequence of  $\pi$ -pulses whose interval fluctuates with variance  $\alpha = 0.25$  is also applied on spin 2. We finally measure the amplitude of spin 1 at  $t = T$ . We repeat the measurement by preparing 128 series of variables  $\{\Xi_1, \Xi_2, \dots, \Xi_{128}\}$  as input parameters. The magnitude of averaged amplitude is plotted as a function of  $T$  in Fig. 7. The correspondence between the symbol and the bang-bang pulse interval is ( $\square$  :  $t_b = 0.50$  ms), ( $\circ$  :  $t_b = 0.67$  ms), ( $\triangle$  :  $t_b = 1.00$  ms). The broken line in Fig. 7 is the reference data with regular pulses on spin 2 and no pulses on spin 1, as shown in Fig. 5 (a). The solid line in Fig. 7 is the experimental result with random pulses on spin 2 and without the bang-bang control to spin 1 (Fig. 5 (b)). Comparing the data points  $\{\square\}$  with the solid line, we observe that decoherence is suppressed

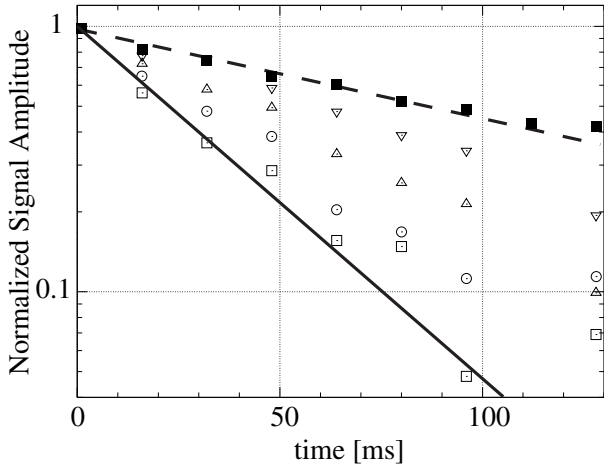


FIG. 6: Time evolution of  $|a_x + ia_y|$  of spin 1. Decrease of these magnitude implies phase decoherence. The correspondence between the symbol and the variance  $\alpha$  of the pulse interval distribution is ( $\blacksquare$  :  $\alpha = 0$ ), ( $\nabla$  :  $\alpha = 0.10$ ), ( $\triangle$  :  $\alpha = 0.15$ ), ( $\circ$  :  $\alpha = 0.20$ ) and ( $\square$  :  $\alpha = 0.25$ ). The broken line is the least square fit for  $\{\blacksquare\}$  while the solid line is that for  $\{\square\}$ .

by the bang-bang control. The decoherence factor is read from  $\{\square\}$  in Fig. 7 as

$$e^{-T/T_2^*} = 0.35 \text{ at } T = 60 \text{ ms for } t_b = 0.50 \text{ ms.} \quad (69)$$

The decoherence factor of the reference broken line in Fig. 7 is

$$e^{-T/T_2^*} = 0.63 \text{ at } T = 60 \text{ ms for } \alpha = 0. \quad (70)$$

Their ratio is

$$\frac{e^{-T/T_2^*}|_{\text{bang}}}{e^{-T/T_2^*}|_{\text{ref}}} = \frac{0.35}{0.63} = 0.56. \quad (71)$$

On the other hand, the theoretical prediction (62) gives

$$e^{-T/T_2^*}|_{\text{theory}} = 0.56. \quad (72)$$

This estimation therefore agrees with the observed result (71).

As a final step, we conduct an experiment depicted in Fig. 5 (d) in which the bang-bang control to spin 1 is applied with no random pulses applied to spin 2. We measure amplitudes of spin 1 FID and the results are shown in Fig. 7. The correspondence between the symbol and the bang-bang pulse interval is ( $\blacksquare$  :  $t_b = 0.50$  ms), ( $\bullet$  :  $t_b = 1.00$  ms), ( $\blacktriangle$  :  $t_b = 2.00$  ms). The plotted points are close to the broken reference line. Here we observe that decoherence becomes slightly faster as we let the interval  $t_b$  shorter. A possible account of this result is that accumulation of bang-bang pulse imperfection may cause

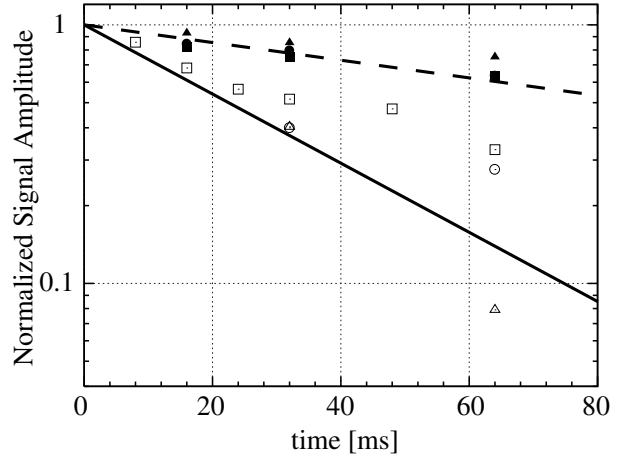


FIG. 7: The magnitude  $|a_x + ia_y|$  of spin 1 with the bang-bang control applied. The broken line and the solid line are the same as in Fig. 6. Series of  $\pi$ -pulses with variance  $\alpha = 0.25$  is applied to spin 2. The correspondence between the symbol and the bang-bang time interval is ( $\square$  :  $t_b = 0.50$  ms), ( $\circ$  :  $t_b = 0.67$  ms) and ( $\triangle$  :  $t_b = 1.00$  ms). Measurements are also made without pulse application to spin 2 as depicted in Fig. 5 (d). The correspondence is ( $\blacksquare$  :  $t_b = 0.50$  ms), ( $\bullet$  :  $t_b = 1.00$  ms) and ( $\blacktriangle$  :  $t_b = 2.00$  ms).

the faster decoherence. In contrast, decoherence is slower if we choose smaller  $t_b$  in experiment in which random pulses are applied on spin 2. From these results we conclude that the bang-bang pulses have suppressed decoherence of a dynamical origin. This should be compared with cancellation of static field inhomogeneity using conventional spin-echo method in NMR [23]. Needless to say, bang-bang pulses also cancel decoherence of static origin of this kind.

## VI. CONCLUSION

We have shown in this paper that a two-qubit system can simulate a composite of a system (qubit 1) and an environment (qubit 2) so that qubit 1 exhibits phase decoherence, provided that the state of qubit 2 is randomized by external manipulation. We have evaluated decoherence rates of qubit 1 and also shown that decoherence is suppressed by applying the bang-bang control to qubit 1.

Performing NMR experiments with a two-spin molecule we measured decoherence in a clear manner. In the simulation of phase decoherence in a qubit flying through a quantum transmission line, our theoretical calculations were consistent with the measured ampli-

tudes. In the simulation of phase decoherence of a quantum memory, our theoretical calculations qualitatively explained the measured decoherence rates. It was confirmed that the decoherence rate  $(T_2^*)^{-1}$  is proportional to the squared variance  $\alpha^2$  of the interval distribution of the pulses applied to the environment (qubit 2). In both cases we demonstrated that the bang-bang control, successive time reversal operations of which interval is much shorter than the correlation time of the artificial environment, successfully suppressed decoherence.

Study of a qubit system as a composite of a system and an environment will help our understanding of the mechanism of decoherence and will help further development of techniques to suppress decoherence.

## Acknowledgments

We would like to thank Paolo Zanardi for giving us a series of lectures on quantum theory of open systems. MN would like to thank Mikko Paalanen and Jukka Pekola for warm hospitality extended to him during his stay at Low Temperature Laboratory, Helsinki University of Technology, Finland, where a part of this work was done. ST is partially supported by JSPS, Grant Nos. 15540277 and 17540372.

---

[1] M. A. Nielsen and I. L. Chuang, *Quantum Computation and Quantum Information* (Cambridge University Press, Cambridge, 2000).

[2] L. M. K. Vandersypen, M. Steffen, G. Breyta, C. S. Yannoni, M. H. Sherwood, and I. L. Chuang, *Nature* **414**, 883 (2001).

[3] R. Fitzgerald, *Physics Today*, **53**, No. 1, 20 (2000).

[4] M. Nakahara, Y. Kondo, K. Hata, and S. Tanimura, *Phys. Rev. A* **70**, 052319 (2004).

[5] M. Nakahara, J. J. Vartiainen, Y. Kondo, S. Tanimura, and K. Hata, *Phys. Lett. A* **350**, 27 (2006).

[6] P. Zanardi, *Phys. Rev. A* **56**, 4445 (1997); *Phys. Rev. A* **57**, 3276 (1998).

[7] M. Ban, *J. Mod. Opt.* **45**, 2315 (1998); L. Viola and S. Lloyd, *Phys. Rev. A* **58**, 2733 (1998); L. Duan and G. Guo, *Phys. Lett. A* **261**, 139 (1999); L. Viola, E. Knill, and S. Lloyd, *Phys. Rev. Lett.* **82**, 2417 (1999); L. Viola, S. Lloyd, and E. Knill, *Phys. Rev. Lett.* **83**, 4888 (1999); L. Tian and S. Lloyd, *Phys. Rev. A* **62**, 050301(R) (2000). See, also, H. Gutmann, F. K. Wilhelm, W. M. Kaminsky, and S. Lloyd, *Bang-Bang Refocusing of a Qubit Exposed to Telegraph Noise in Experimental Aspects of Quantum Computing*, edited by H. O. Everitt (Springer, New York, 2005).

[8] C. Uchiyama and M. Aihara, *Phys. Rev. A* **66**, 032313 (2002); *Phys. Rev. A* **68**, 052302 (2003).

[9] T. Kohmoto, Y. Fukuda, M. Kunitomo, K. Ishikawa, Y. Takahashi, K. Ebina, and M. Kaburagi, *Phys. Rev. B* **52**, 13475 (1995).

[10] K.-E. Hellwig and K. Kraus, *Commun. Math. Phys.* **11**, 214 (1969).

[11] K. Kraus, *Ann. Phys.* **64**, 311 (1971).

[12] E. C. G. Sudarshan, P. M. Mathews and J. Rau, *Phys. Rev.* **121**, 920 (1961).

[13] D. Leung, L. Vandersypen, X. Zhou, M. Sherwood, C. Yannoni, M. Kubinec, and I. Chuang, *Phys. Rev. A* **60**, 1924 (1999).

[14] P. W. Anderson, *J. Phys. Soc. Jpn.* **9**, 316 (1954); R. Kubo, *J. Phys. Soc. Jpn.* **9**, 935 (1954); R. Kubo, in *Fluctuation, Relaxation and Resonance in Magnetic Systems*, ed. by ter Haar (Oliver and Boyd, Edinburgh, 1962); R. Kubo and N. Hashitsume, *Statistical Physics II, Nonequilibrium Statistical Mechanics* (Springer-Verlag, Berlin, Heidelberg, New York, Tokyo, 1985).

[15] W. H. Zurek, *Phys. Rev. D* **26**, 1862 (1982).

[16] J. Zhang, Z. Lu, L. Shan, and Z. Deng, arXiv: quant-ph/0202146; quant-ph/0204113.

[17] G. Teklemariam, E. M. Fortunato, C. C. López, J. Emerson, J. P. Paz, T. F. Havel, and D. G. Cory, *Phys. Rev. A* **67**, 062316 (2003).

[18] R. R. Ernst, *J. Chem. Phys.* **45**, 3845 (1966).

[19] S. Kitajima, M. Ban, and F. Shibata, No. 25aYG12 in the 60th annual meeting of the Physical Society of Japan (2005).

[20] D. Pines and P. Slichter, *Phys. Rev.* **100**, 1014 (1955).

[21] <http://www.jeol.com/>.

[22] U. Sakaguchi, H. Ozawa, and T. Fukumi, *Phys. Rev. A* **61**, 042313 (2000).

[23] M. H. Levitt, *Spin Dynamics* (John Wiley and Sons, New York, 2001).